THE JOURNAL OF PHYSICAL CHEMISTRY A

Article

pubs.acs.org/JPCA

Rate Constant and Thermochemistry for K + O_2 + N_2 = KO_2 + N_2

Tapio Sorvajärvi,[†] Jan Viljanen,[†] Juha Toivonen,[†] Paul Marshall,*[,‡] and Peter Glarborg[§]

[†]Optics Laboratory, Department of Physics, Tampere University of Technology, P.O. Box 692, FI-33101 Tampere, Finland

[‡]Department of Chemistry and Center for Advanced Scientific Computing and Modeling (CASCaM), University of North Texas, 1155 Union Circle #305070, Denton, Texas 76203−5017, United States

[§]Department of Chemical and Biochemical Engineering, Technical University of Denmark, DK-2800 Kgs. Lyngby, Denmark

Supporting Information

ABSTRACT: The addition reaction of potassium atoms with oxygen has been studied using the collinear photofragmentation and atomic absorption spectroscopy (CPFAAS) method. KCl vapor was photolyzed with 266 nm pulses and the absorbance by K atoms at 766.5 nm was measured at various delay times with a narrow line width diode laser. Experiments were carried out with O_2/N_2 mixtures at a total pressure of 1 bar, over 748−1323 K. At the lower temperatures single exponential decays of [K] yielded the third-order rate constant for addition, k_{R1}, whereas at higher temperatures equilibration was observed in the form of double exponential decays of [K], which yielded both k_{R1} and the equilibrium constant for KO_2 formation. k_{R1} can be summarized as $1.07 \times 10^{-30}(T/1000\ \mathrm{K})^{-0.733}$ cm^6 molecule^{-2} s^{-1}. Combination with literature values leads to a recommended k_{R1} of $5.5 \times 10^{-26}T^{-1.55}\exp(-10/T)$ cm^6 molecule^{-2} s^{-1} over 250−1320 K, with an error limit of a factor of 1.5. A van't Hoff analysis constrained to fit the computed ΔS_{298} yields a K−O_2 bond dissociation enthalpy of 184.2 ± 4.0 kJ mol^{-1} at 298 K and $\Delta_f H_{298}(KO_2) = -95.2 \pm 4.1$ kJ mol^{-1}. The corresponding D_0 is 181.5 ± 4.0 kJ mol^{-1}. This value compares well with a CCSD(T) extrapolation to the complete basis set limit, with all electrons correlated, of 177.9 kJ mol^{-1}.

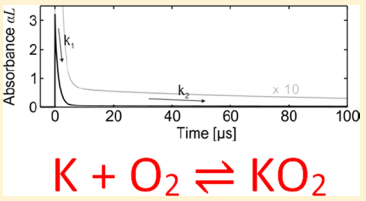

INTRODUCTION

The high-temperature chemistry of alkali metal species has important implications for combustion. It is well established that the presence of alkali metal species may result in flame inhibition[1,2] and alkali-based flame inhibitors are of interest.[3,4] Potassium additives are also known to have an impact on gun muzzle flash.[5] Furthermore, most solid fuels contain alkali metals in minor quantities. Biomass such as wood and annual crops releases potassium to the vapor phase during pyrolysis and combustion,[6−8] mainly in the form of KCl. Once released, the alkali metal chlorides may be partially converted to alkali metal hydroxide or alkali metal sulfates.[9] During cooling, the alkali metal components will condense, contributing to aerosol formation and/or cause operational problems, such as deposit formation and corrosion in boilers.[10,11] The fate of the alkali metal will depend on interactions with the sulfur and chlorine species of the gas.

Formation of potassium superoxide, KO_2, is potentially important for both flame inhibition and the high-temperature K/S/Cl transformation in combustion. The ability of alkali metals to catalyze radical removal is well documented by data from laminar premixed flames[12−25] and flow reactor experiments.[26] Alkali-metal-based flame inhibitors are typically added as particulates[3,4] and heterogeneous effects have been proposed; however, the inhibiting effect of alkali metals is attributed mostly to gas phase radical removal reactions. The mechanism of inhibition is still in discussion. Under reducing conditions, results from flames[16,17,21] and from flow reactors[26] are consistent with the sequence (for K): KOH/KCl + H → K + H_2O/HCl, K + OH + M → KOH + M. In combustion systems, alkali metal chlorides and alkali metal hydroxides are rapidly equilibrated through the fast reaction KCl + H_2O ⇌ KOH + HCl.[9] Under lean conditions, the inhibition mechanism is more uncertain. The chain-terminating recombination reaction,

$$K + O_2 + M \rightleftharpoons KO_2 + M \qquad (R1)$$

has been suggested to be important.[18,27−29] However, it has been questioned whether potassium superoxide was sufficiently stable to play an important role under flame conditions.[2,26]

Formation of alkali metal superoxides (mainly KO_2) may also play a role in the gas-phase transformation of alkali metal, sulfur, and chlorine species in solid fuel combustion. Provided KO_2 is sufficiently stable, it could promote oxidation of SO_2 to SO_3 through the reaction $SO_2 + KO_2 \rightarrow SO_3 + KO$, which has been estimated to be fast.[30]

The importance of KO_2 in combustion depends on the rate constant for K + O_2 + M (R1) and on the thermal stability of KO_2. Values of k_{R1} have been measured directly in the temperature range 250−1100 K,[31−34] inferred from studies of lean premixed flames,[27−29] and calculated theoretically.[35] The direct measurements are in reasonably good agreement but deviate significantly from the values derived at high temperatures from flames. Also the thermochemistry of KO_2 is in

Received: January 24, 2015
Revised: March 14, 2015
Published: March 16, 2015

DOI: 10.1021/acs.jpca.5b00755
J. Phys. Chem. A 2015, 119, 3329−3336

discussion. Values for the bond dissociation energy D_0 of KO_2 have been inferred from flame studies,[18,36] a molecular beam study,[37] time-resolved decay of atomic potassium,[34] and from theory.[34,38−40] Although recent theoretical studies imply a value of the BDE of approximately 172 ± 4 kJ mol^{-1},[38−40] some data inferred from experiment indicate a substantially larger value.[34,37]

The objective of the present work is to extend the measurement range for the rate constant for K + O_2 + N_2 to higher temperatures compared to previous direct studies, and to provide the first direct measurements of the bond dissociation energy of KO_2. For this purpose we use the recently developed optical technique called collinear photofragmentation and atomic absorption spectroscopy (CPFAAS). This technique is based on the fragmentation of a precursor molecule and the detection of the fragment atoms via absorption spectroscopy.[41,42] It has been applied to monitor concentrations of the precursors KCl and KOH in combustion during combustion of solid biomass fuels,[43] but to our knowledge the present work is its first application to chemical kinetics. Previous CPFAAS studies have focused on the maximum absorbance right after the photofragmentation that is proportional to the precursor molecule concentration. The decay process of the induced K atoms has been assumed to be exponential and was not studied in detail. In the present work, measurements analogous to CPFAAS experiments are performed to study the decay process of [K] in the temperature range of 748−1323 K and in atmospheres containing O_2 from 40 ppm to 21.4%.

EXPERIMENTAL SECTION

Potassium atoms were produced and detected using a measurement setup presented in Figure 1. The K atoms were formed through photofragmentation of KCl molecules in an 80 cm long quartz sample tube having an inner diameter of 35 mm. The KCl powder was brought into the middle of the cell in a 10 cm long glazed combustion boat. The temperature of the sample tube was adjusted with a 50 cm long and 30 cm wide tube oven. The gas atmosphere in the tube was adjusted by flushing the tube for 5 min before each experiment with a gas mixture prepared by diluting dry synthetic air with nitrogen using a mass flow controller (5850S, Brooks Instruments). A gas flow of 2 standard liters per minute (L min^{-1}) was brought to the tube from the entrance side of the probe laser and 0.2 L min^{-1} from the exhaust side of the tube. The small flow at the exhaust side prevented the deposition of the KCl vapor on the inner surface of the exit window of the cell. The gas flows were closed 2 min before recording the decay of the K atoms. The sample was at atmospheric pressure during the measurement.

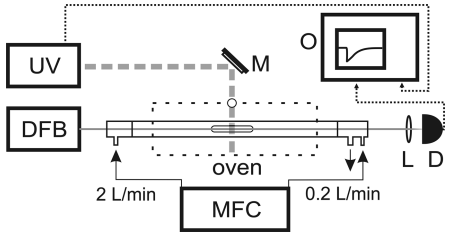

Figure 1. Experimental setup for the time-resolved detection of photoinduced potassium atoms: photofragmentation laser (UV); probe laser (DFB); mirror (M); lens (L); detector (D); oscilloscope (O); mass flow controller (MFC).

The dissociation of the KCl molecules was performed by applying a fragmentation laser (FQSS 266-200, Crylas GmbH). It emitted 1 ns long pulses with a 20 Hz repetition rate at a wavelength of 266 nm. The laser pulses entered the sample tube through an 18 mm hole at the side of the oven and through the wall of the tube. The transmission of the wall material for the fragmentation wavelength was measured to be approximately 80%. The pulse energies of the fragmentation laser in the sample tube were adjusted to between 1 and 80 μJ, and the cross sectional 1/e diameter of the pulses was adjusted over the range of 3−10 mm, such that detected probe beam transmission did not drop to zero. The energy densities of the UV pulses in the tube were smaller than the saturation intensity of KCl.[44] The pulses were slightly focused with a lens prior to the entrance hole to increase the concentration of the released K atoms at the lower temperatures (<873 K) when the vapor pressure of KCl was small. The pulses traveled 10 mm above the top of the combustion boat and were dumped to the back wall of the oven.

The relative concentration of the K atoms was measured by applying a narrow line width distributed feedback diode laser (Nanoplus GmbH), which emitted light at a wavelength of 766.5 nm (in air). The wavelength of the diode laser was locked to the absorption line of K atoms in a reference cell (SC-K-19 × 75-Q-W, Photonics Technologies).[42] The probe beam having a 1/e diameter of 1 mm was aligned to travel through the tube and to cross the volume affected by the fragmentation pulses. The optical path of the probe laser beam and the fragmentation pulses were perpendicular to each other in the tube. The short interaction region meant that the temperature was constant across it, despite any overall temperature gradients along the entire sample tube. The induced K atoms decreased the transmission intensity of the probe beam temporarily. The transmission waveform caused by the photofragmentation was detected using an amplified photodiode (PDA10A, Thorlabs) and a 12-bit oscilloscope (HDO6054, LeCroy).

An example waveform measured at a temperature of 1173 K in 2.67% of O_2 is presented in Figure 2a. The photofragmentation of KCl molecules took place at t = 0, and it is seen as a fast dip in the photodiode (PD) voltage due to the temporarily increased absorption by the K atoms. The fragmentation was followed by recovery of the transmission as the induced K atoms reacted with ambient gas molecules and the distorted gas volume approached equilibrium.

To study the recovery process of the concentration of K atoms, the PD voltage was converted to the absorbance αL by applying the Beer−Lambert law,

$$\alpha L = -\ln[I(t)/I(t<0)] \quad (1)$$

Figure 2b shows the corresponding absorbance curve calculated using eq 1. The absorbance is directly proportional to the sample concentration and the conversion can be done when absorption length and absorption cross section are known. The effective absorption length in this measurement was 1 cm (UV beam diameter) and the absorption cross section of K atoms at the wavelength in question is 1.25 × 10^{-16} m^2,[43] which converts an absorbance equal to 1 to a K concentration of 130 ppb. At the lower end of the temperature range studied, the absorbance was observed to follow a single exponential decay,

$$\alpha L(t>0) = A_1 \exp(-k_1 t) \quad (2)$$

DOI: 10.1021/acs.jpca.5b00755
J. Phys. Chem. A 2015, 119, 3329−3336

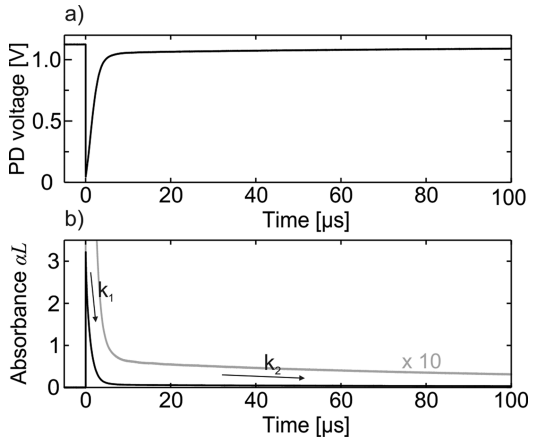

Figure 2. (a) Probe laser transmission curve. The dip is caused by the photofragmentation of KCl molecules. (b) Corresponding absorbance curve calculated from the transmission curve. The induced absorbance decays with two rate constants k_1 and k_2. The second phase decay is emphasized in (b) by magnifying the decay curve by a factor of 10. The experiment was done at a temperature of 1173 K in 2.67% of O_2 in N_2.

whereas at higher temperatures a double exponential decay process was observed,

$$\alpha L(t>0) = A_1 \exp(-k_1 t) + A_2 \exp(-k_2 t) \quad (3)$$

RESULTS AND DISCUSSION

At 1073 K and below simple exponential kinetics were observed, in the form of eq 2, which may be interpreted in terms of the scheme

$$K + O_2 \xrightarrow{k_a} KO_2 \quad (a)$$

$$K \xrightarrow{k_d} \text{loss} \quad (d)$$

k_a represents the effective second-order forward rate constant for reaction R1 and k_d accounts for loss of K atoms by processes that do not involve oxygen, such as diffusion. One would therefore expect the variation of potassium concentration with time t to follow eq 4,

$$[K] = [K]_0 \exp(-k_1 t) \quad (4)$$

where $k_1 = k_a[O_2] + k_d$. Figure 3 shows a plot of k_1 vs $[O_2]$, from which it may be seen that the expected linear dependence on $[O_2]$ from reaction (a) is exhibited, and that the intercept is negligible, so that on the short time scale of these experiments k_d is indistinguishable from zero. Details of k_1 and $[O_2]$ measurements are provided in the Supporting Information (Table S1), and the results for the third-order rate constant k_{R1} derived as the slope k_a divided by $[O_2] + [N_2]$ (corresponding to 1 bar total pressure) for 873−1073 K are listed in Table 1. Approximate, purely statistical, error limits were assessed via twice the standard deviation of the slopes of plots like Figure 3. At 748, 773, and 823 K single measurements of k_1 were made, and divided by $[O_2]$ and $[O_2] + [N_2]$ to obtain k_{R1}. We allow 25% error limits for these points, and also for a single measurement at 1323 K where black liquor (alkali-metal-rich waste product from pulp and paper processing) rather than KCl was the source of K atoms.

We now turn to the measurements made at the higher temperatures where double-exponential decays of absorbance

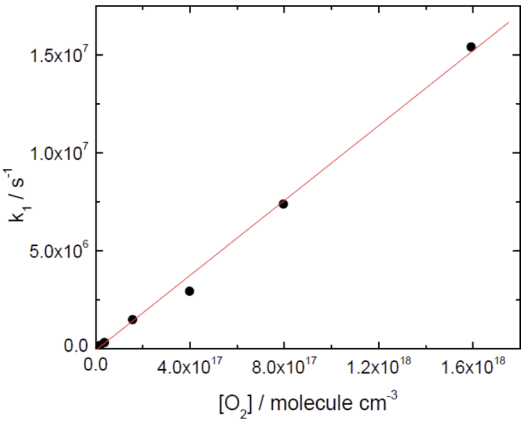

Figure 3. Exponential decay coefficient for potassium atoms as a function of oxygen concentration at 923 K and a total pressure of 1 bar made up with nitrogen.

Table 1. Summary of Measurements for K + O_2 + N_2

T/°C	T/K	$(k_{R1} \pm 2\sigma)/10^{-30}$ cm^6 molecule^{-2} s^{-1}	comment
475	748	1.47 ± 0.37	single point
500	773	1.31 ± 0.33	single point
550	823	1.24 ± 0.31	single point
600	873	1.18 ± 0.16	exponential decays
650	923	1.15 ± 0.04	exponential decays
700	973	1.07 ± 0.02	exponential decays
750	1023	0.998 ± 0.027	exponential decays
800	1073	0.789 ± 0.140	exponential decays
800	1073	0.978 ± 0.152	equilibrium mechanism
850	1123	0.982 ± 0.024	equilibrium mechanism
900	1173	0.969 ± 0.032	equilibrium mechanism
950	1223	0.973 ± 0.063	equilibrium mechanism
1000	1273	1.01 ± 0.07	equilibrium mechanism
1050	1323	0.919 ± 0.230	single point, black liquor

were seen. Figure 4 shows a temporal K concentration profile upon photofragmentation of the KCl molecules at a temperature of 1223 K in 10.7% O_2. In agreement with the results of Figure 2, [K] is observed to recover to its original level in two steps. In the first phase [K] decreases fast and the 1/e relaxation time constant $1/k_1$ is found to be 270 ns (Figure 4a). Figure 4b shows how [K] does not recover fully in the first phase and saturates to a nonzero level. Figure 4c presents how the second phase relaxation takes place on a time scale of the order of 100 μs. The 1/e decay time constant for the second phase relaxation was, in the example signal, $1/k_2$ = 40 μs.

This double-exponential behavior, quantified in the form of eq 3, can be observed when reactants reversibly form an intermediate, and a reactant and/or intermediate is also lost irreversibly.[45] In the absence of oxygen the lifetime of K was observed to be of the order of 1 ms, where K atoms are lost presumably mainly by diffusion out of the probe laser beam. This lifetime is too long to be significant on the time scale of the K atom profiles when O_2 is present. Accordingly, we have interpreted the results in terms of a simple mechanism

$$K + O_2 \xrightarrow{k_a} KO_2 \quad (a)$$

$$KO_2 \xrightarrow{k_{-a}} K + O_2 \quad (-a)$$

DOI: 10.1021/acs.jpca.5b00755
J. Phys. Chem. A 2015, 119, 3329−3336

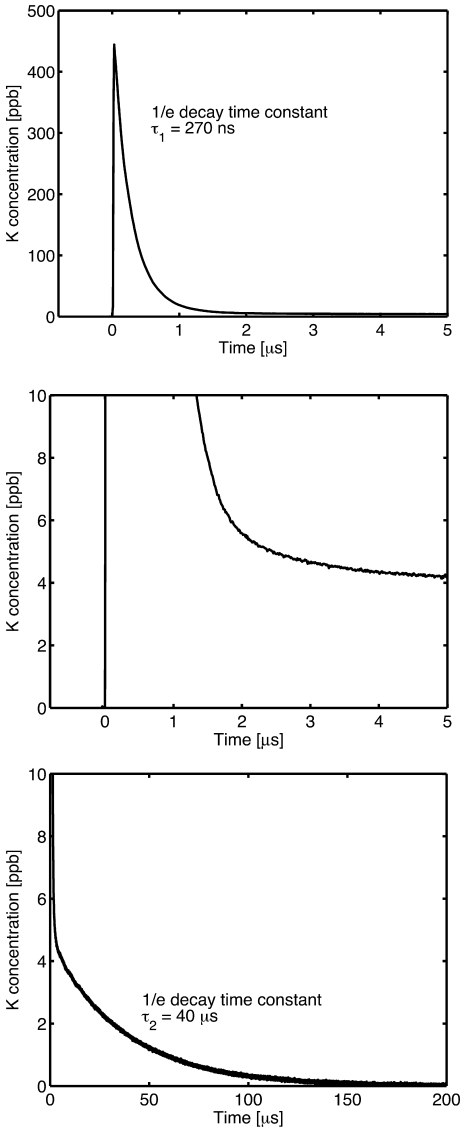

Figure 4. K relaxation after KCl photofragmentation at a temperature of 1223 K in 10.7% O_2: (a) first phase relaxation; (b) The concentration of K does not reach the original background level within first 5 μs. (c) The thermodynamic equilibrium [K] is reached 200 μs after the fragmentation. $[K]_0$ is the potassium concentration right after the photofragmentation, and $[K]_0^{res}$ is the concentration of the residual potassium atoms. This value is calculated by extrapolating the second phase recovery to $t = 0$. $\tau_1 = 1/k_1$ and $\tau_2 = 1/k_2$ are the recovery time constants in the fitting equation $[K]_t = ([K]_0 - [K]_0^{res}) \exp(-t/\tau_1) + [K]_0^{res} \exp(-t/\tau_2)$.

$$KO_2 \xrightarrow{k_b} \text{loss} \quad \text{(b)}$$

k_a represents the effective second-order rate constant for K atom addition to O_2 at a given total pressure, k_{-a} is the effective first-order dissociation rate of KO_2, and k_b is the effective first-order rate of loss of KO_2 by pathways that do not regenerate K atoms. These include diffusive loss of KO_2 although presumably this is even slower than the neglected diffusive loss of K atoms. Assuming $[O_2] \gg [K]_0$, the integrated rate law may be written as[45]

$$[K] = \frac{[K]_0}{\lambda_1 - \lambda_2}((Q + \lambda_1)e^{\lambda_1 t} - (Q + \lambda_2)e^{\lambda_2 t}) \quad (5)$$

with

$$Q = k_{-a} + k_b \quad (6)$$

$$\lambda_1 + \lambda_2 = -Q - k_a[O_2] \quad (7)$$

$$\lambda_1\lambda_2 = k_b k_a[O_2] \quad (8)$$

By comparing terms with the empirical eq 3, we see that the three rate constants may be derived via

$$[K]_0 = A_1 + A_2 \quad (9)$$

$$Q = k_1 + \frac{A_1(k_2 - k_1)}{[K]_0} \quad (10)$$

$$k_a[O_2] = k_1 + k_2 - Q \quad (11)$$

$$k_b = \frac{k_1 k_2}{k_a[O_2]} \quad (12)$$

$$k_{-a} = Q - k_b \quad (13)$$

This analysis was applied to the double exponential data obtained over 1073−1273 K. A check on the consistency of the analysis is that the $k_a[O_2]$ term should vary linearly with $[O_2]$ and k_{-a} should be independent of $[O_2]$. Figure 5 shows the

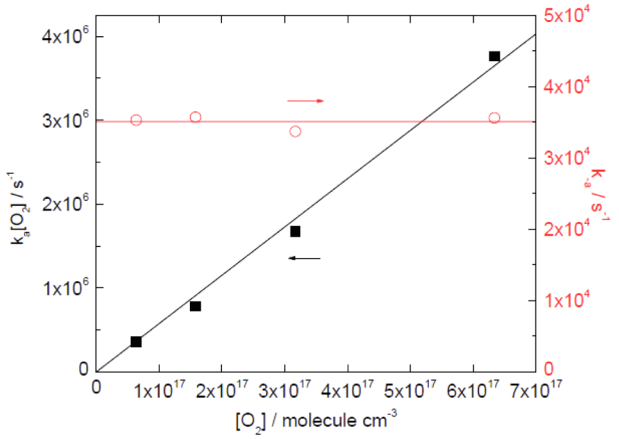

Figure 5. Effective first-order rate constants at 1223 K for K addition to O_2 (solid black squares, left axis, linear fit constrained to pass through the origin) and for KO_2 dissociation (open red circles, right axis, linear fit constrained to have zero slope).

results at 1223 K, and it may be seen that these conditions are met. A second check is that at 1073 K, low $[O_2]$ led to double-exponential behavior whereas at high $[O_2]$ the equilibrium is shifted sufficiently toward products that the back-reaction is negligible, leading to single exponential decays of [K]. Data obtained both ways are tabulated for comparison, but unfortunately, at this temperature neither method works very well because $k_a[O_2]$ and k_{-a} are not well-separated. The results are given in Table S1 (Supporting Information) where we report the slope of $k_a[O_2]$ vs $[O_2]$ plots constrained to pass through the origin, and the mean of the k_{-a} values. Again, k_{R1} is obtained by dividing k_a by $[N_2] + [O_2] \approx [N_2]$ and is listed in Table 1.

The present rate constants can be summarized as $k_{R1} = 1.07 \times 10^{-30}(T/1000\ \text{K})^{-0.733}$ cm^6 molecule^{-2} s^{-1} over 750−1320 K. They are in reasonable accord with the prior determinations up to 1100 K plotted on Figure 6 but the rate coefficients do not

DOI: 10.1021/acs.jpca.5b00755
J. Phys. Chem. A 2015, 119, 3329−3336

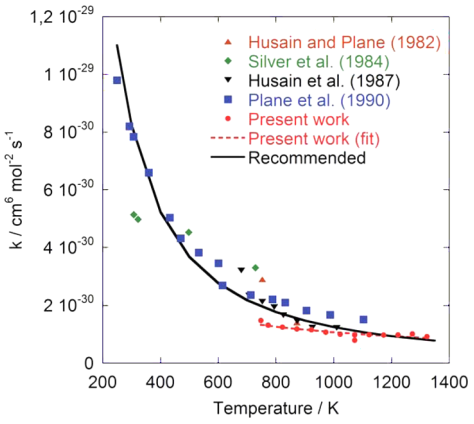

Figure 6. Arrhenius plot for the reaction K + O_2 + N_2 ⇌ KO_2 + N_2. The symbols denote the experimental data from Husain and Plane,[32] Silver et al.,[31] Husain et al.,[33] Plane et al.[34] and from the present work. The dashed line shows a best fit to the present data (k_{R1} = 1.07 × $10^{-30}(T/1000\ K)^{-0.733}$ cm^6 $molecule^{-2}$ s^{-1} (750−1320 K), and the solid line shows the recommended k_{R1} of 5.5 × $10^{-26}T^{-1.55}$ exp(−10/T) cm^6 $molecule^{-2}$ s^{-1} over 250−1320 K.

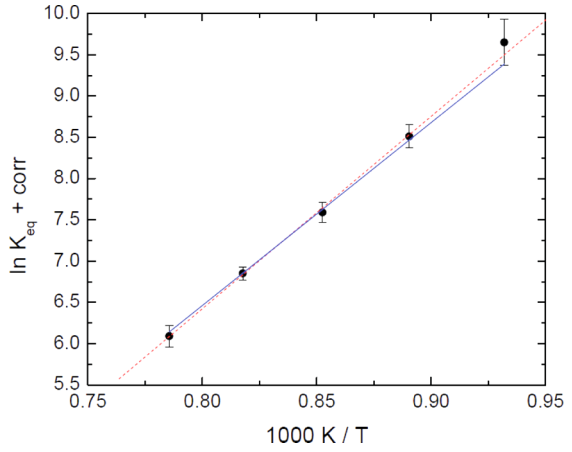

Figure 7. van't Hoff plot of K_{eq} for K + O_2 ⇌ KO_2. A second-law fit is shown as the dashed red line and a third-law fit is shown as the solid blue line.

extrapolate well to lower temperatures. An overall fit to the data of the present work together with those of Husain and Plane,[32] Husain et al.,[33] and Plane et al.[34] leads to a recommended k_{R1} of 5.5 × $10^{-26}T^{-1.55}$ exp(−10/T) cm^6 $molecule^{-2}$ s^{-1} over 250−1320 K. An error limit of a factor of 1.5 includes most of the present and past measurements.

The ratio k_a/k_{-a} equals the concentration equilibrium constant K_c, which is listed in Table 2, along with the thermodynamic equilibrium constant K_{eq} based on unit activity for a standard pressure of 1 bar. A van't Hoff plot for K_{eq} yields thermodynamic information for reaction R1. A potential complication is the temperature dependence of ΔH and ΔS. A correction term to ln K_{eq} of $(\Delta H_T - \Delta H_{298})/RT - (\Delta S_T - \Delta S_{298})/R$ was added so that the slope and intercept of the van't Hoff plot in Figure 7 correspond to $-\Delta H_{298}/R$ and $\Delta S_{298}/R$, respectively. This small correction was derived via statistical mechanics from the experimental properties of K and O_2,[46] the KO_2 vibrational frequencies of 1109, 307, and 304 cm^{-1} [47] and the ab initio C_{2v} geometry of Vasiliu et al.,[40] a K−O distance of 2.40 × 10^{-10} m, and a OKO angle of 32.5°. The correction varied from −0.016 at 1073 K to −0.031 at 1323 K. The unconstrained linear fit corresponds to a second-law analysis and yields ΔS_{298} = −101.7 ± 9.9 J K^{-1} mol^{-1} and ΔH_{298} = −193.8 ± 11.9 kJ mol^{-1}. The error limits are 2σ and are purely the statistical uncertainty of the fit. A third-law analysis constrains the intercept to the separately estimated ΔS_{298} = 93.6 J K^{-1} mol^{-1} and yields ΔH_{298} = −184.2 ± 0.5 kJ mol^{-1}. The thermodynamic parameters agree between both methods, but as expected, the third-law method is more precise. Combined with $\Delta_f H_{298}$ = 89.0 ± 0.8 kJ mol^{-1} for atomic potassium,[46] the corresponding heat of formation of KO_2 is $\Delta_f H_{298}$ = −95.2 ± 4.1 kJ mol^{-1}. The experimental vibrational frequencies for KO_2 yield $H_{298} - H_0$ = 12.14 kJ mol^{-1}, and together with $H_{298} - H_0$ of 6.20 and 8.68 kJ mol^{-1} for K and O_2, respectively,[46] we obtain the 0 K bond strength D_0(K−O_2) as 181.5 kJ mol^{-1}. This value is compared with experimental and theoretical results from the literature in Table 3.

Table 2. Equilibrium Constants Derived from Forward and Reverse Kinetics (See Text)

T/K	$K_c/10^{-16}$ cm^3 $molecule^{-1}$	K_{eq} std state 1 bar	correction[a]	ln(K_{eq}) + corr	σ[b]
1073	23.5	1.59 × 10^4	−0.016	9.65	0.28
1123	7.87	5.08 × 10^3	−0.017	8.51	0.14
1173	3.28	2.03 × 10^3	−0.021	7.59	0.12
1223	1.64	971	−0.027	6.85	0.08
1273	0.799	455	−0.031	6.09	0.13

[a]Equal to $(\Delta H_T - \Delta H_{298})/RT - (\Delta S_T - \Delta S_{298})/R$. [b]Statistical uncertainty in ln(K_{eq}).

Table 3. Reported Bond Dissociation Energies for KO_2 and Comparison with the Present Values

reference	D_0/kJ mol^{-1}	method
Jensen[36]	170 ± 30	flame study
Figger et al.[37]	188 ± 10	molecular beam study
Hynes et al.[18]	174 ± 20	flame study
Plane et al.[34]	≥203	time resolved decay (LIF)
Plane et al.[34]	154	theory
Partridge et al.[38]	170 ± 8	theory
Lee and Wright[39]	168 ± 3	theory
Vasiliu et al.[40]	173	theory
Present work	181.5 ± 4	CPFAAS
Present work	177.9	theory

There remains the issue of systematic error. A rough-and-ready approach is based on the ca. factor of 1.5 differences between literature determinations of k_a which, if propagated as a factor of 1.5 variation in K_{eq}, imply a variation of ±4 kJ mol^{-1} in ΔH_{298}. With this as an uncertainty limit, the 298 K bond strength is 8.7 kJ mol^{-1} above that calculated by Vasiliu et al.[40] and is therefore significantly different.

AB INITIO ANALYSIS

It is common to exclude core electrons from the correlation treatment in ab initio analysis. For a potassium atom, these would be the 1s, 2s, 2p, 3s, and 3p orbitals. However, in an ionic compound like KO_2 the potassium loses its only valence 4s electron so the remaining interactions involve the core electrons. Indeed, the 3s and 3p atomic orbitals may be higher in energy than the oxygen orbitals. For this reason it has become standard practice in calculations on alkali metals to

DOI: 10.1021/acs.jpca.5b00755
J. Phys. Chem. A 2015, 119, 3329−3336

Table 4. Computed Reaction Enthalpies at 0 K in the KO_2 System, with Contributions from Each Term, in kJ mol^{-1}

reaction	Δ(CCSD(T)/aug-cc-pwCVQZ)	Δ(CCSD(T)/aug-cc-pwCV5Z)	ΔE_{inf}	ΔE_{zpe}	ΔE_{rel}	ΔE_{final}
D_0(ions)	555.32	556.27	557.27	−3.92	0.91	553.35[a]
D_0	175.64	177.96	180.39	−1.11	−1.36	177.92
IP(K)	416.58	416.67	416.76	0.00	1.39	418.15
−EA(O_2)	−36.91	−38.36	−39.88	−2.81	0.88	−42.73[a]

[a]Includes empirical −0.91 kJ mol^{-1} correction to the energy of O_2^- for splitting in its $^2\Pi$ ground state.[53]

incorporate some of these inner orbitals in the correlation space[48] and, in particular, Vasilu et al.[40] included the 3s and 3p electrons in their correlation treatment at the coupled cluster level, CCSD(T), for potassium compounds.

In this work the geometries of O_2, O_2^-, and KO_2 were obtained using coupled cluster theory and the large aug-cc-pwCVQZ atomic basis set for oxygen[49] and specially constructed for potassium by Peterson and co-workers,[50] with all the electrons correlated. The optimized O−O distances in the three molecules are 0.121, 0.135, and 0.135 nm, consistent with a $K^+O_2^-$ species where there is charge transfer to the oxygen. In KO_2 the computed K−O distance is 0.240 nm. Then single-point energies were derived with CCSD(T)/aug-cc-pwCV5Z theory,[50] again with all electrons correlated, followed by a scalar relativistic correction Erel (mass-velocity plus Darwin terms) performed at the CISD/aug-cc-pwCVQZ level of theory. These calculations were made with the Molpro 2010 program,[51] and the results are listed in Table S2 (Supporting Information). The CCSD(T) results with ζ = 4 and 5 were extrapolated to the infinite basis set limit via the relation:[52]

$$E_{inf} = (125 \cdot E_5 - 64 \cdot E_4)/61 \quad (14)$$

Vibrational zero-point energies E_{zpe} were derived from experimental data (KO_2;[47] O_2 and O_2^-[53]). The final energies (E_{inf} + E_{rel} + E_{zpe}) were employed to derive 0 K enthalpy changes for the reactions in Table 4, which are coupled via the Hess cycle

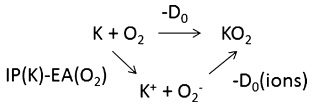

It may be seen that that the ionization potential of K is close to converged with the aug-cc-pwCVQZ basis set and that the final extrapolation is very small, only 0.09 kJ mol^{-1}, and with the relativistic correction we compute IP(K) = 418.15 kJ mol^{-1}, which is 0.66 kJ mol^{-1} below the experimental value of 418.81 kJ mol^{-1}.[56] Similarly, the dissociation enthalpy of KO_2 to ions is nearly converged with the ζ = 4 basis set. The other two processes involve extrapolations of only ca. 2 kJ mol^{-1} so application of different extrapolation strategies would have little impact on ΔE_{final}. The direct calculation of D_0 yields 177.9 kJ mol^{-1}, which is somewhat larger than the 172.8 kJ mol^{-1} derived by Vasiliu et al.[40] using a similar computational method. The critical difference may be the use of a frozen inner core of electrons in the prior work vs the all-electron calculations here. The 5 kJ mol^{-1} increase in D_0 more closely brings theory and experiment, 184.2 ± 4.0 kJ mol^{-1}, into accord. The electron affinity of oxygen is reproduced well at the present level of theory, which yields EA(O_2) about 0.7 kJ mol^{-1} too low when compared to the experimental value of 43.38 ± 0.18 kJ mol^{-1}.[54,55] A similar modest error might exist in KO_2 where a superoxide moiety is present. An alternative assessment of D_0 is thus equal to D_0(ions) − IP(K) + EA(O_2). With experimental values for the latter two items, this also yields D_0 = 177.9 kJ mol^{-1}, confirming the calculation via neutrals. The errors in IP(K) and EA(O_2) have canceled.

CONCLUSIONS

The collinear photofragmentation and atomic absorption spectroscopy (CPFAAS) method has been applied to generate and monitor atomic potassium in the presence of oxygen. Rate constants for the third-order addition process were determined over 748−1323 K, which compare well with prior data obtained at up to 1100 K. The short time scale of the detection method permits direct observation of equilibration in the K + O_2 = KO_2 system for the first time. A third-law analysis yields the K−O_2 bond dissociation enthalpy, which is 9 kJ mol^{-1} greater than the most recent ab initio calculations in the literature. We find that correlating all the electrons in coupled cluster/infinite basis set calculations roughly halves the discrepancy.

ASSOCIATED CONTENT

Supporting Information

Supplementary Table S1 reports the results of the kinetic analyses for K atom loss in the presence of oxygen in a nitrogen bath gas. Supplementary Table S2 summarizes ab initio energies of K, O_2, KO_2, K^+, and O_2^-. This material is available free of charge via the Internet at http://pubs.acs.org.

AUTHOR INFORMATION

Notes

The authors declare no competing financial interest.

ACKNOWLEDGMENTS

We thank Prof. K. A. Peterson (Washington State University) for providing the potassium basis sets. This work has been partly carried out within CLIFF (2014-2017) as part of the activities of Tampere University of Technology. Other research partners are Åbo Akademi University, VTT Technical Research Centre of Finland, Lappeenranta University of Technology, and Aalto University. Support from the National Technology Agency of Finland (Tekes), Andritz Oy, Valmet Technologies Oy, Foster Wheeler Energia Oy, UPM-Kymmene Oyj, Clyde Bergemann GmbH, International Paper Inc., and Top Analytica Oy Ab is gratefully acknowledged. P.M. thanks the Robert A. Welch Foundation (Grant B-1174) for support. P.G. acknowledges financial support by the Danish Strategic Research Council (GREEN).

REFERENCES

(1) Dautriche, H. The Effect of Alkaline Salts with a Fixed Base on the Combustion of Gases and the Combustible Thrust. *Compt. Rend.* **1908**, *146*, 535.

(2) Glarborg, P. Hidden Interactions - Trace Species Governing Combustion and Emissions. *Proc. Combust. Inst.* **2007**, *31*, 77−98.

(3) Mitani, T.; Niioka, T. Extinction Phenomenon of Premixed Flames with Alkali Metal Compounds. *Combust. Flame* **1984**, *55*, 13−21.

DOI: 10.1021/acs.jpca.5b00755
J. Phys. Chem. A 2015, 119, 3329−3336

(4) Kim, H.-T. Inhibition Effectiveness of Dry Chemical in Methane/Air Flames. *Korean J. Chem. Eng.* **1992**, *9*, 1−7.
(5) Klingenberg, G.; Heimerl, J. M. Gun Muzzle Blast and Flash. *Prog. Astronaut. Aeronaut* **1992**, *139*, 241−260.
(6) van Lith, S. C.; Ramirez, V. A.; Jensen, P. A.; Frandsen, F. J.; Glarborg, P. Release to the Gas Phase of Inorganic Elements during Wood Combustion. Part 1: Development and Evaluation of Quantification Methods. *Energy Fuels* **2006**, *20*, 964−978.
(7) van Lith, S. C.; Jensen, P. A.; Frandsen, F. J.; Glarborg, P. Release to the Gas Phase of Inorganic Elements during Wood Combustion. Part 2: Influence of Fuel Composition. *Energy Fuels* **2008**, *22*, 1598−1609.
(8) Knudsen, J. N.; Jensen, P. A.; Dam-Johansen, K. Transformation and Release to the Gas Phase of Cl, K, and S during Combustion of Annual Biomass. *Energy Fuels* **2004**, *18*, 1385−1399.
(9) Glarborg, P.; Marshall, P. Mechanism and Modeling of Gaseous Alkali Sulfate Formation. *Combust. Flame* **2005**, *141*, 22−39.
(10) Christensen, K. A.; Livbjerg, H. A Field Study of Submicron Particles from the Combustion of Straw. *J. Aerosol Sci.* **1996**, *25*, 185−199.
(11) Christensen, K. A.; Stenholm, M.; Livbjerg, H. The Formation of Submicron Aerosol Particles, HCl and SO_2 in Straw-Fired Boilers. *J. Aerosol Sci.* **1998**, *29*, 421−444.
(12) Rosser, W. A., Jr.; Inami, S. H.; Wise, H. The Effect of Metal Salts on Premixed Hydrocarbon-Air Flames. *Combust. Flame* **1963**, *7*, 107−119.
(13) Dewitte, M.; Vrebosch, M.; van Tiggelen, J. A. Inhibition and Extinction of Premixed Flames by Dust Particles. *Combust. Flame* **1964**, *8*, 257.
(14) Hoffmann, W. Influence of Alkali Metal Salts on Laminar Flame Velocity. *Chem. Ing. Tech.* **1971**, *43*, 556−560.
(15) Iya, K. S.; Wollowitz, S.; Kaskan, W. E. The Mechanism of Flame Inhibition by Sodium Salts. *Proc. Combust. Inst.* **1975**, *15*, 329−336.
(16) Jensen, D. E.; Jones, G. A.; Mace, A. C. H. Flame Inhibition by Potassium. *J. Chem. Soc., Faraday Trans 1* **1979**, *75*, 2377−2385.
(17) Jensen, D. E.; Jones, G. A. Kinetics of Flame Inhibition by Sodium. *J. Chem. Soc., Faraday Trans. 1* **1982**, *78*, 2843−2850.
(18) Hynes, A. J.; Steinberg, M.; Schofield, K. The Chemical Kinetics and Thermodynamics of Sodium Species in Oxygen-rich Hydrogen Flames. *J. Chem. Phys.* **1984**, *80*, 2585−2597.
(19) Kim, H. T.; Reuther, J. J. Temperature Dependence of Dry Chemical Premixed Flame Inhibition Effectiveness. *Combust. Flame* **1984**, *57*, 313−317.
(20) Bulewicz, E. M.; Kucnerowicz-Polak, B. J. The Action of Sodium-Bicarbonate and of Silica Powder on Upward Propagating Flame in a Vertical Duct. *Combust. Flame* **1987**, *70*, 127−135.
(21) Slack, M.; Cox, J. W.; Grillo, A.; Ryan, R.; Smith, O. Potassium Kinetics in Heavily Seeded Atmospheric-Pressure Laminar Methane Flames. *Combust. Flame* **1989**, *77*, 311−320.
(22) Steinberg, M.; Schofield, K. The Chemistry of Sodium with Sulfur in Flames. *Prog. Energy Combust. Sci.* **1990**, *16*, 311−317.
(23) Schofield, K.; Steinberg, M. Sodium Sulfur Chemical Behavior in Fuel-Rich and Fuel-Lean Flames. *J. Chem. Phys.* **1992**, *96*, 715−726.
(24) Babushok, V.; Tsang, W.; Linteris, G. T.; Reinelt, D. Chemical Limits to Flame Inhibition. *Combust. Flame* **1998**, *115*, 551.
(25) Williams, B. A.; Fleming, J. W. CF_3Br and Other Suppressants: Differences in Effects on Flame Structure. *Proc. Combust. Inst.* **2002**, *29*, 345−351.
(26) Hindiyarti, L.; Frandsen, F.; Livbjerg, H.; Glarborg, P. Influence of Potassium Chloride on Moist CO Oxidation under Reducing Conditions: Experimental and Kinetic Modeling Study. *Fuel* **2006**, *85*, 978−988.
(27) Kaskan, W. E. The Reaction of Alkali Atoms in Lean Flames. *Proc. Combust. Inst.* **1965**, *10*, 41−46.
(28) McEwan, M. J.; Phillips, L. F. Dissociation Energy of NaO_2*. *Trans. Faraday Soc.* **1966**, *62*, 1717−1720.
(29) Carabetta, R.; Kaskan, W. E. The Oxidation of Sodium, Potassium, and Cesium in Flames. *J. Phys. Chem.* **1968**, *72*, 2483−2489.
(30) Hindiyarti, L.; Frandsen, F.; Livbjerg, H.; Glarborg, P.; Marshall, P. An Exploratory Study of Alkali Sulfate Aerosol Formation during Biomass Combustion. *Fuel* **2008**, *87*, 1591−1600.
(31) Silver, J. A.; Zahniser, M. S.; Stanton, A. C.; Kolb, C. E. Temperature Dependent Termolecular Reaction Rate Constants for Potassium and Sodium Superoxide. *Proc. Combust. Inst.* **1984**, *20*, 605−612.
(32) Husain, D.; Plane, J. M. C. Kinetic Investigation of the Third-order Rate Process between K + O_2 + M by Time-Resolved Atomic Resonance Absorption Spectroscopy. *J. Chem. Soc., Faraday Trans. 2* **1982**, *78*, 1175−1194.
(33) Husain, D.; Lee, Y. H.; Marshall, P. Temperature Dependence of the Absolute Third-Order Rate Constant for the Reaction between K + O_2 + M over the Range 680−1010 K Studied by Time-Resolved Atomic Resonance Absorption Spectroscopy. *Combust. Flame* **1987**, *68*, 143−154.
(34) Plane, J. M. C.; Rajasekhar, B.; Bartolotti, L. Kinetic Study of the Reaction K + O_2 + M (M = N_2, He) from 250 to 1103 K. *J. Phys. Chem.* **1990**, *94*, 4161−4167.
(35) Patrick, R.; Golden, D. M. Termolecular Reactions of Alkali Metal Atoms with O_2 and OH. *Int. J. Chem. Kinet.* **1984**, *16*, 1567−1574.
(36) Jensen, D. E. Alkali Metal Compounds in Oxygen-Rich Flames - A Reinterpretation of Experimental Results. *J. Chem. Soc., Faraday Trans.* **1982**, *178*, 2835−2842.
(37) Figger, H.; Schrepp, W.; Zhu, X. Chemiluminescent Reaction between Alkali Dimers and Oxygen Molecules. *J. Chem. Phys.* **1983**, *79*, 1320.
(38) Partridge, H.; Bauschlicher, C. W., Jr.; Sodupe, M.; Langhoff, S. R. Theoretical Determination of the Alkali-metal Superoxide Bond Energies. *Chem. Phys. Lett.* **1992**, *195*, 200−206.
(39) Lee, E. P. F.; Wright, T. G. The Ionization Energy of KO_2 (X^2A_2) and Dissociation Energies of KO_2 and KO_2^+. *Chem. Phys. Lett.* **2002**, *363*, 139−144.
(40) Vasiliu, M.; Li, S.; Peterson, K. A.; Feller, D.; Gole, J. L.; Dixon, D. A. Structures and Heats of Formation of Simple Alkali Metal Compounds: Hydrides, Chlorides, Fluorides, Hydroxides, and Oxides for Li, Na, and K. *J. Phys. Chem. A* **2010**, *114*, 4272−4281.
(41) Sorvajärvi, T.; Saarela, J.; Toivonen, J. Optical Detection of Potassium Chloride Vapor using Collinear Photofragmentation and Atomic Absorption Spectroscopy. *Opt. Lett.* **2012**, *37*, 4011−4013.
(42) Sorvajärvi, T.; Toivonen, J. Principles and Calibration of Collinear Photofragmentation and Atomic Absorption Spectroscopy. *Appl. Phys. B: Laser Opt.* **2014**, *115*, 533−539.
(43) Sorvajärvi, T.; DeMartini, N.; Rossi, J.; Toivonen, J. In Situ Measurement Technique for Simultaneous Detection of K, KCl, and KOH Vapors Released During Combustion of Solid Biomass Fuel in a Single Particle Reactor. *Appl. Spectrosc.* **2014**, *68*, 179−187.
(44) Sorvajärvi, T.; Manninen, A.; Toivonen, J.; Saarela, J.; Hernberg, R. Resonant Photoacoustic Cell for Pulsed Laser Analysis of Gases at High Temperature. *Rev. Sci. Instrum.* **2009**, *80*, 123103.
(45) Ayhens, Y. V.; Nicovich, J. M.; McKee, M. L.; Wine, P. H. Kinetic and Mechanistic Study of the Reaction of Atomic Chlorine with Methyl Iodide over the Temperature Range 218−694 K. *J. Phys. Chem. A* **1997**, *101*, 9382−9390.
(46) The Computational Chemistry Comparison and Benchmark Database (CCCBDB), Web site http://cccbdb.nist.gov/.
(47) Tremblay, B.; Manceron, L.; Roy, P.; LeQuéré, A.-M.; Roy, D. Vibrational Spectra and Structure of the KO_2 Complex in Solid Argon - A Far-Infrared Study. *Chem. Phys. Lett.* **1994**, *228*, 410−416.
(48) Iron, M. A.; Oren, M.; Martin, J. M. L. Alkali and Alkaline Earth Metal Compounds: Core-Valence Basis Sets and Importance of Subvalence Correlation. *Mol. Phys.* **2003**, *101*, 1345−1361.
(49) Dunning, T. H., Jr. Gaussian-Basis Sets for Use in Correlated Molecular Calculations. 1. The Atoms Boron through Neon and Hydrogen. *J. Chem. Phys.* **1989**, *90*, 1007.

DOI: 10.1021/acs.jpca.5b00755
J. Phys. Chem. A 2015, 119, 3329−3336

(50) Peterson, K. A. Private communication.
(51) Werner, H.-J.; Knowles, P. J.; Lindh, R.; Manby, F. R.; Schutz, M.; Celani, P.; Korona, T.; Mitrushenkov, A.; Rauhut, G.; Adler, T. B.; et al. *Molpro Quantum Chemistry Package* **2009**, http://www.molpro.net/.
(52) Halkier, A.; Helgaker, T.; Jorgensen, P.; Klopper, W.; Koch, H.; Olsen, J.; Wilson, A. K. Basis-Set Convergence in Correlated Calculations on Ne, N_2, and H_2O. *Chem. Phys. Lett.* **1998**, *286*, 243−252.
(53) Ervin, K. M.; Anusiewicz, I.; Skurski, P.; Simons, J.; Lineberger, W. C. The Only Stable State of O_2^- Is the X $^2\Pi_g$ Ground State and It (Still!) Has an Adiabatic Electron Detachment Energy of 0.45 eV. *J. Phys. Chem. A* **2003**, *107*, 8521−8529.
(54) Ruscic, B.; Pinzon, R. E.; Morton, M. L.; von Laszewski, G.; Bittner, S.; Nijsure, S. G.; Amin, K. A.; Minkoff, M.; Wagner, A. F. Introduction to Active Thermochemical Tables: Several "Key" Enthalpies of Formation Revisited. *J. Phys. Chem. A* **2004**, *108*, 9979−9997.
(55) Ruscic, B.; Pinzon, R. E.; von Laszewski, G.; Kodeboyina, D.; Burcat, A.; Leahy, D.; Montoya, D.; Wagner, A. F. Active Thermochemical Tables: Thermochemistry for the 21st Century. *J. Phys. Conf. Ser.* **2005**, *16*, 561−570.
(56) NIST Chemistry WebBook, webbook.nist.gov/chemistry/.

DOI: 10.1021/acs.jpca.5b00755
J. Phys. Chem. A 2015, 119, 3329−3336